Open Access Research Journal of
Chemistry and Pharmacy
Journals home page: https://oarjpublication/journals/oarjcp/
ISSN: 2783-0276 (Online)

OARJ OPEN ACCESS RESEARCH JOURNALS

(RESEARCH ARTICLE)

Isotherm, kinetic and thermodynamic of arsenic adsorption from aqueous solution using *Theobroma cacao* pod-modified feldspar composite

Yakubu Yahaya [1,*], Kabir A Sanusi [1,2], Murtala M Ambrusa [1] and Aminu Koko Rabiu [1]

[1] *Department of Pure and Applied Chemistry, Kebbi State University of Science and Technology Aliero in Kebbi State, Nigeria.*
[2] *Department of Chemical Sciences, Federal University of Kashere, P. M. B. 0182, Gombe State, Nigeria.*

Open Access Research Journal of Chemistry and Pharmacy, 2021, 01(01), 013–032

Publication history: Received on 21 February 2021; revised on 20 March 2021; accepted on 23 March 2021

Article DOI: https://doi.org/10.53022/oarjcp.2021.1.1.0026

Abstract

In this study modified feldspar composite (MFC) adsorbent based on feldspar and *Theobroma cacao* pods (TCP) was prepared using calcination method, characterized and tested for the removal As (III) from aqueous solution. The results showed that the cation exchange capacity of the modified feldspar composite (30.66 ± 0.21 meq/100 g) was 5 times higher than that of raw feldspar (6.42 ± 0.45 meq/100g). More so, the novel biohybrid material, MFC has a surface area of 53.60 ± 0.3 m^2/g and particle size of 105.4 ± 0.18. Response surface methodology (RSM) via central composite design (CCD) was utilized in the optimization of the efficiency of As (III) ions uptake by the novel composite (MFC) in 20 experiment runs. The optimization results revealed that predicted adsorption percentages of (99.72%) for As (III) ions was close to the experimental results (99.98%) for the metal ions at the optimum conditions of adsorption parameters (pH 5; 0.5 g; 100 mg/L; 120 min and 328^{0}K). The adequacy and validation of the model was justified with the good agreement between R^2 values (0.9959) and adjusted R^2 (0.9981) and higher F values (≥ 147) from the analysis of variance (ANOVA) results. Furthermore, the results from isotherm studies showed that As (III) ions adsorption onto the adsorbent best fitted the Langmuir isotherm model, hence chemisorption process. The results of the kinetic studies showed that the rate of uptake of As (III) ions onto MFC active sites followed pseudo second order kinetic model. The Intraparticle diffusion though not the only rate - controlling step, played an important role in the metal ions uptake by the adsorbent. The thermodynamic results revealed that As (III) adsorption onto MFC surface was feasible, spontaneous with negative ΔH values, suggestive of exothermic process. The MFC, owing to its abundance and other properties as its improved cation exchange capacity and eco-friendliness has a good potential as a highly efficient alternative adsorbent to commercial activated carbons in water treatment.

Keywords: *Theobroma cacao;* Adsorption; Response surface methodology; As (III); CCD

1. Introduction

Water is an essential resource for life which greatly influences public and environmental health as well as a requirement for domestic, irrigation and industrial activities (Francis, 2018). Industries in developed and developing countries in recent times have faced a lot of problems due to improper disposal of their metallic-laden effluents. These have resulted in emerging contaminants in water bodies causing severe health implications even at low metal concentrations (Mustapha *et al*., 2019). Effluents from industries such as tanning, mining, microelectronics, electroplating, battery manufacture, fertilizer, pharmaceutical and inputs from other anthropogenic activities have contributed to the increase in contaminated waters all over the globe (Jimoh *et al.,* 2011).

Among the potentially toxic elements, heavy metals such as arsenic, mercury, cadmium, chromium, lead and palladium are not biodegradable, persistent and tend to accumulate in living organisms, causing different health disorders in

* Corresponding author: Yakubu Yahaya
Department of Pure and Applied Chemistry, Kebbi State University of Science and Technology Aliero in Kebbi State, Nigeria.

human depending on the exposure rate and dosage (Dang *et al*., 2009). Direct toxicity to man and other forms of life and indirect toxicity through the food chains are the focus of this concern (Horsefall *et al*., 2004).

Trivalent arsenic is about 60 times more toxic than arsenic in the oxidized pentavalent state. Permanent arsenic intake can lead to chronic intoxication, and prolonged arsenic exposure can damage the central nervous system, liver, and skin and results in the appearance of diverse types of cancers, such as hyperkeratosis, lung, skin, and prostate cancers (Chiban *et al.,* 2012). Therefore, it is a necessity to maintain the water quality by reducing the heavy metal ion concentrations, especially when higher than the permissible limits to make them fit for human consumption and other purposes (Mustapha *et al*., 2019).

To alleviate the problem of water pollution by heavy metals, various conventional methods including precipitation, coagulation, floatation, adsorption, ion exchange, reverse osmosis, ultrafiltration, electro-dialysis and membrane filtration processes have been used. However, most of these methods of water treatment suffer several techno-economic limitations such as inefficiency, cost expensive, sludge production, membrane instability (Dang *et al.,* 2009).

Removal of toxic chemical substances by adsorption using low-cost adsorbents is a latest method of choice in the water treatment due to several techno-economic advantages associated with low-cost adsorbents and environmental friendly (Olu-Owolabi *et al*., 2016). Among available natural materials, clays, siliceous materials and agrowastes are regarded as good adsorbents because they are non-toxic, abundant, environmentally friendliness and multi-functional group properties. A number of researchers have utilized wide variety of clays for adsorption experiments. A number of researchers have utilized natural materials such as sepiolite (Brigatti *et al.,* 2011), kaolinite (Unuabonah *et al.,* 2007), feldspar (Awala and El-Jamal, 2011, Sanusi *et al*., 2016), bentonite (Olu-Owolabi *et al*., 2016), Manisonia wood sawdust (Ofomoja *et al.,* 2010), *Carica papaya* seed (Sanusi *et al*., 2015), mango seed and cocoa pod waste (Olu-Owolabi *et al.,* 2012) in water pollution management.

Recently, a modification method involving synergistic combination of aluminosilicate materials and agricultural wastes (both being low cost adsorbents) are beginning to receive attention for subsequent improvement in adsorption capacity and efficiency of the new composite adsorbents produced (Unuabonah et al., 2013; Ogbu et al., 2018). Modified feldspar composite exploits the advantage of the adsorption characteristics of each material that yield the novel composite. Such synergistic combinations lead to better adsorbent properties such as high cation exchange capacity (CEC), elimination of bleeding, good adsorption efficiency and larger surface area and comparatively low-cost for water treatment.

This study utilized the potential of *Theobroma cacao* Pod-Modified Feldspar Composite (MFC) for the removal of As (III) ions from aqueous solution with the optimization of adsorption parameters. Furthermore, the isotherm, kinetic and thermodynamic of As (III) ions onto MFC adsorbent was investigated.

2. Material and methods

2.1. Collection and preparation of Adsorbents

The *Theobroma cacao* (Cocoa) pods (TCP) were collected from cocoa plantations in Ifetedo town, Osun State. The samples were washed thoroughly with tap water dust and dirt and then distilled water to impurities, oven-dried at 70^0C for 72h, ground into powder, sieved in a 0.230 mm sieve and stored in a pre-cleaned dry air-tight plastic container (Olu-Owolabi *et al*., 2010; Sanusi *et al.,* 2016).

The feldspar (FS) sample was obtained from the Federal Institute of Industrial Research Oshodi (FIIRO), Lagos, Nigeria. The sample was pre-treated by suspension in deionized water for 24 h and the suspension was carefully decanted to obtain the feldspar (Unuabonah *et al*., 2013). The sample was oven dried at 105 ^{0}C, ground into powder, sieved through a 0.230 mm mesh size sieve and stored in a pre-cleaned dry air-tight plastic container for subsequent studies (Adebowale *et al.,* 2005; Sanusi *et al*., 2016).

For the preparation of modified feldspar composite (MFC), equal weight of feldspar sample and *Theobroma cacao* pods (50 g each) were weighed into a 500 mL beaker and 300 mL of 0.1M NaOH was added, thoroughly stirred, oven-dried at 150 ^{o}C and then calcined at 300 ^{o}C for 6 h (Olu-Owolabi *et al*., 2016). The resulting dark powdery composite was washed with deionized water to remove residual NaOH from its surface, oven-dried at 105^{o}C and referred to as Modified Feldspar Composite (MFC) Adsorbent (Unuabonah *et al.,* 2013).

2.2. Characterization of adsorbents

The cation exchange capacity (CEC) of MFC was determined using the ammonium acetate method as reported by Unuabonah *et al*. (2013). Na^+ and K^+ were determined using AES (Agilent PG 10T), while Ca^{2+} and Mg^{2+} were determined by atomic absorption spectrophotometer (SHIMAZU 360H Model). The summation of the exchangeable cations (Ca^{2+}, Mg^{2+}, Na^+, and K^+) gave the cation exchange capacity (CEC). (Unuabonah *et al.,* 2013).

The functional groups present in the adsorbent (MFC) was obtained using Shimadzu 8400S FTIR spectrometer operating on Platinum-Attenuated Total Reflectance (ATR) method and recorded in the frequency range of 4000 - 400 cm^{-1} (Adebowale *et al.,* 2005, Singh and Bhateria, 2020).

The surface morphology of the MFC adsorbent was analyzed using scanning electron microscopy (SEM), Philips XL30 model. After gold coating (Philip J1050 sputter coater), the micrograph of the MFC was scanned and recorded at 32 scan and 15keV (Hossain, 2013; Dawood, 2018).

2.3. Preparation of As (III) stock solution

A stock solution of (1000 mg/L) of As^{3+} was prepared by dissolving 1.320 g of arsenic trioxide (As_2O_3) in 200 cm^3 deionized water containing 1M NaOH solution. The was made up to the mark in a 1L standard volumetric flask. Working solutions of various As^{3+} concentrations were prepared from the stock solution by serial dilution (Chiban *et al.,* 2007).

2.4. Batch Adsorption Experiment

Batch metal adsorption experiments were carried out in 100mL plastic bottles by contacting 0.5 g of adsorbents with 20 mL of As (III) solution of 100mg/L concentration. pH adjustments was done with either 0.1M NaOH or 0.1M HCl to a pH 5±0.2 (Chukwuemeka-Okorie et al., 2018). The adsorbent/metal ion mixtures were placed on a rotary shaker and shaken at 120 rpm at a room temperature (300^0K) for a period of 120 min to attain equilibrium (Anusa et al., 2017). The effect of adsorption parameters such as contact time (15-300 min) and adsorbate concentration (50-300 mg/L) and temperature (308-328 ^{0}K) were investigated for As (III) ions onto the MFC adsorbent. On completion of experimental time, the sample mixtures were filtered using whatman 0.45µm filter paper and the filtrate were analyzed for the concentration of the As (III) left in solution using hydride generation-atomic absorption spectrophotometric method (AAS-50HT Agilent Model). All adsorption experiments were carried out in triplicates (Unuabonah *et al.,* 2013; Anusa *et al.,* 2017).

2.4.1. Optimization of Adsorption Parameters

Design-Expert 12 software ("MiniTab" version 15) was applied in the design of experiment using central composite design. In the design process, three adsorption variables were considered for optimization, viz; As (III) concentrations (50-150 mg/L) and contact time (30-210 min) and temperature as a function of the efficiency of MFC for As (III) ion adsorption (response).

Number of experiments (N) = $(2^n+2n+n_c) = 2^3 + (2\times3) + 6 = 20$ runs

Table 1 Adsorption parameters (Independent variables) and their corresponding coded levels

Independent variables		**Ranges and Coded Levels**			
	- α	**-1**	**0**	**+1**	**+ α**
Initial metal conc. (C_0) (mg/L)	50	75	100	125	150
Temperature (K) (g)	300	308	315	318	328
Contact time (T)(min)	30	60	120	180	210

2.4.2. Determination of effect of interaction of adsorption variables

A quadratic model in form of expression below was developed for the adsorption of As (III) ions as it was influenced by the adsorption variables considered during the experiments. The response model may be represented as

$$Y = \beta_0 + \sum_{i=1}^{n} \beta_i X_i + \sum_{i=1}^{n} \beta_{ii} X_i^2 + \sum_{i=1}^{n-1} \sum_{j=i+1}^{n} \beta_{ij} X_i X_j, \quad (1)$$

where Y is the response, and the objective is to optimize the response (Y). β_0 is the constant coefficient, is β_i the linear coefficients, β_{ii} is the quadratic coefficients, β_{ij} is the interaction coefficients, and X_i and X_j are the coded values of the independent process variables. Coefficient of determination (R^2) was used to determine the quality of the model as it compared the data from predicted model with data got from experimental runs (Yazdani *et al.,* 2013; Adetokun *et al.,* 2018).

2.5. Data Treatment

2.5.1. Calculation of the removal of metal ions by MFC

The amount of heavy metals ions adsorbed per gram was calculated using the equation 2.

$$q_e = \frac{(C_O - C_e)V}{M} \qquad 2$$

where; C_O and C_e are the initial and final metal ion concentrations in solutions; q_e, V and M are the amount of metal ions adsorbed (mg/g), volume of the solution (mL) used for experiment and mass (g) of sample, respectively.

2.6. Calculation of the percentage metal ions removed by MFC

The percentage removal of heavy metal ions was calculated using the equation 3.

$$\%R = \frac{C_O - C_e}{C_o} \times 100 \qquad 3$$

Where; R is the removal efficiency of the metal ions adsorbent studied; C_O is the initial metal ions concentration in solution (mg/L); C_e is the metal ions concentration removed or adsorbed by adsorbent at equilibrium (mg/L).

2.6.1. Adsorption Isotherm Models

The relationship between the amount of As (III) ions adsorbed onto MFC adsorbent and the equilibrium concentrations in aqueous solution were evaluated using of Langmuir and Freundlich models.

The Langmuir isotherm is represented by the equation 4.

$$q_e = \frac{Q_O b C_e}{1 + b C_e} \qquad 4$$

or its linear form in equation 5.

$$\frac{C_e}{q_e} = \frac{1}{Q_o b} + \frac{C_e}{Q_o} \qquad 5$$

When $\frac{C_e}{q_e}$ is plotted against C_e, the slope is equal to $\frac{1}{Q_o}$ and the intercept is equal to $\frac{1}{Q_o b}$

The essential characteristics of the Langmuir isotherm can be expressed in terms of a dimensionless constant separation factor or equilibrium parameter (RL) which is defined by:

$R_L = 1/ (1 + b\, C_0)$ 6

Where *b* is the Langmuir constant and C_0 the highest metal ion concentration (mg/L). The value of R_L indicates the type of the isotherm to be either unfavourable ($R_L > 1$), linear ($R_L = 1$), favourable ($0 < R_L < 1$) or irreversible ($R_L = 0$).

The Freundlich isotherm is represented by equation 7.

$$q_e = K_f C_e^n \quad 7$$

or its linear form in equation 8.

$$\log q_e = \log K_F + \left(\frac{1}{n}\right)\log C_e \quad 8$$

The values of K_f and n may be calculated by plotting log (q_e) versus log (C_e). The slope is equal to $\frac{1}{n}$ and the intercept is equal to log (K_f).

Where Q_o is the maximal adsorption capacity per unit weight of adsorbent, *b* is a solute–surface interaction energy-related parameter, while q_e and C_e are the amount of metal ions adsorbed (mg/g) and metal ions concentrations in solutions after the equilibrium; where K_F and *n* are the Freundlich model capacity factor and the isotherm linearity parameter respectively (Unuabonah *et al*., 2007; Das and Mondal, 2011).

2.6.2. Adsorption Kinetic Models

Four adsorption kinetics models were employed in describing the adsorption experiment data in order to examine the mechanism of the adsorption process. These are the Lagergren pseudo-first-order (PFO), pseudo second-order (PSO), intra-particle diffusion and Elovich models.

The equations are expressed below:

PFO: $$\log(q_e - q_t) = \log q_e - \frac{k_1}{2.303} t \quad 9$$

PSO: $$\frac{t}{q_t} = \frac{1}{k_2 q_e^2} + \frac{t}{q_e} \quad 10$$

Intra-particle diffusion: $$q_t = k_i (t^{1/2}) + C \quad 11$$

Elovich: $$q_t = \frac{1}{\beta} Ln(\alpha\beta) + \frac{1}{\beta} Ln(t) \quad 12$$

where q_e and q_t are adsorption quantity (mg/g) at equilibrium and at time *t*, respectively; k_1 and k_2 are the rate constants (min^{-1}) of the PFO and PSO, respectively; k_i (mg/g/$min^{1/2}$) is the rate parameter of the intra-particle diffusion control stage; α is the initial adsorption rate (mg/g/min) and β is related to the extent of surface coverage and activation energy for chemisorption (g/mg).

The q_e and rate constants were calculated from the slope and intercept of the plots of log *(q_e–q_t) vs. t*; and *t/q vs. t* for PFO and PSO respectively. From equation 10, a plot of q_t vs $t^{1/2}$ should be a straight line with a slope k_i and intercept C when the adsorption mechanism is in line with the intra-particle diffusion process. If the intra-particle diffusion process is the predominant rate-limiting step in the adsorption, the plot would pass through the origin (Olu-Owolabi *et al*., 2016, Sanusi *et al*., 2016).

2.6.3. Thermodynamic parameters

The thermodynamic parameters; enthalpy $\left(\Delta H^{o}\right)$, entropy $\left(\Delta S^{o}\right)$, Gibbs free energy $\left(\Delta G^{o}\right)$ and equilibrium constant (K_C) were evaluated using data from equilibrium metal adsorption studies through following equations:

$$K_C = \frac{C_{ads}}{C_e} \quad 13$$

$$\Delta G^{o} = -RTInK_C \quad 14$$

$$\Delta G° = \Delta H° - T\,\Delta S° \quad \text{.....15}$$

$$\log K_C = -\frac{\Delta H^{o}}{2.303RT} + \frac{\Delta S^{o}}{2.303R} \quad 16$$

Where C_{ads} and C_e are the amount of metal ions adsorbed and the amount remaining in solution after equilibrium; R and T are the universal gas constant (8.314 $Jmol^{-1}K^{-1}$) and the temperature respectively (Adebowale *et al*., 2005).

3. Results and discussion

3.1. Characterization of adsorbents

3.1.1. Cation exchange capacity (CEC)

From the results in Table 2, MFC had the higher value for CEC (30.66 ± 0.21 meq/100g) compared to FS (6.42 ± 0.45 meq/100g). The results indicated that MFC, a composite resulting from the intercalation of FS with TCP has improved ion-exchange capacity from the surface modification process.

Table 2 The pH and Cation Exchange Capacity of the FS and MFC

Adsorbents	**pH**	**Exchangeable cations(meq/100g)**				**CEC (meq/100g)**
		Ca	Mg	K	Na	
FS	4.95±0.36	1.08±0.1	0.45±0.02	3.31±0.4	1.58±0.23	6.42 ± 0.45
MFC	7.60±0.01	5.57±0.9	3.85±0.00	13.88±0.5	7.36±0.99	30.66± 0.21

3.1.2. Fourier Transform Infrared (FTIR) spectroscopy analysis

The infrared spectra of MFC were shown in Figure 1. FTIR spectra of MFC showed several absorption peaks between the scanning frequency ranges of 4000-500 cm^{-1}. The peak exhibit a broad and strong –OH band at 3622 cm^{-1} indicating the presence of hydroxyl, phenolic or carboxylic –OH stretching vibration as typical of cellulose and lignin i.e. free hydroxyl groups in the polysaccharide linkages of TCP wall (Obike et al. (2018); Olu-Owolabi *et al.* (2012b)). The MFC adsorbent, as it could be seen in (Figure 1), has an enhanced absorption bands appearing at 3432 and 3696 cm^{-1} suggestive of vibration bands of TCP (O–H and N–H stretching) overlapping with the adsorption bands of feldspar (–OH stretching of H_2O). The bands at 2928, 2849 cm^{-1} and 1380 cm^{-1} indicating the intercalated TCP (–CH_2 stretching and C–H bending methyl and methylene groups) are present in the spectra of the novel bio-hybrid (MFC) composite (Unuabonah *et al*., 2013). The Si–O bending vibration observed at 1034 cm^{-1} and Al–OH in plane bending vibration at 912 cm^{-1} with significant shift suggesting the peak position is perhaps one of the active sites for interaction of the feldspar with the TCP biomass (Awala and El-Jamal, 2011; Akpomie and Dawodu, 2014b). The intensity of the band at 1626 cm^{-1} of the MFC spectra has increased with a pronounced band shift from the original constituent materials, indicating the first NH–CO group stretching vibration of TCP overlap with –OH bending vibration of H_2O in the interlayer of feldspar. Overall, FTIR spectra revealing –OH bending vibration and the vibration bands of silicates as active sites responsible for binding of metal ions confirmed that the MFC is indeed a composite consisting of feldspar and *Theobroma cacao* pod (Ogbu *et al.,* 2019).

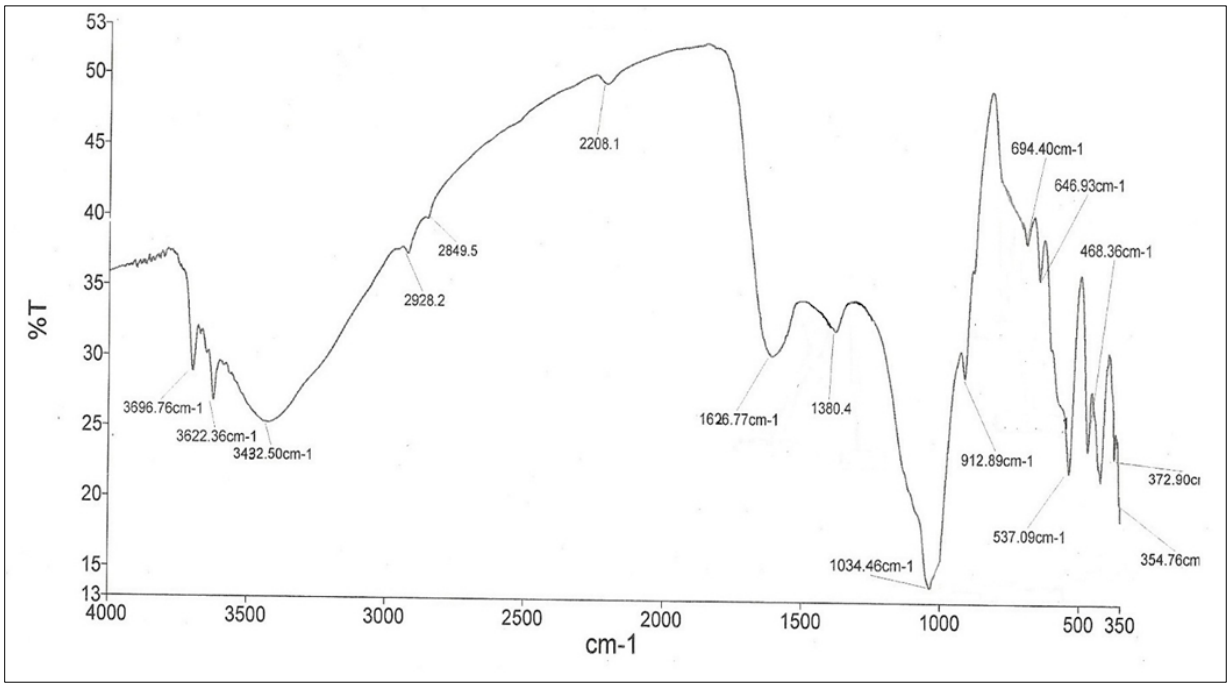

Figure 1 FTIR Spectra of modified feldspar composite (MFC)

3.1.3. SEM Analysis

Figure 2 showed scanning electron microscopy (SEM) of modified feldspar composite (MFC). The SEM micrograph of MFC revealed that the novel composite adsorbent is porous, consisted of considerable number of heterogeneous pores, irregular surface and particle aggregation of various shapes and sizes with relatively flat facets, which is typical of original feldspar mineral (Awala and El-Jamal, 2011 and Ogbu *et al*., 2019). The presence of pores helps in the diffusion of metal ions into the adsorbents during the adsorption of metal ions from solution (Akpomie and Dawodu, 2014b). Also, the SEM image MFC showed some white clumps or particles on the surface, these were probably due to the presence of non-clay minerals like potassium, magnesium, sodium and calcium (Ogbu *et al.,* 2019). From the image of MFC in (Figure 2), it was observed that the bio-based composite is micro porous suitable for As (III) removal from aqueous solutions (Chiban *et al.,* 2012).

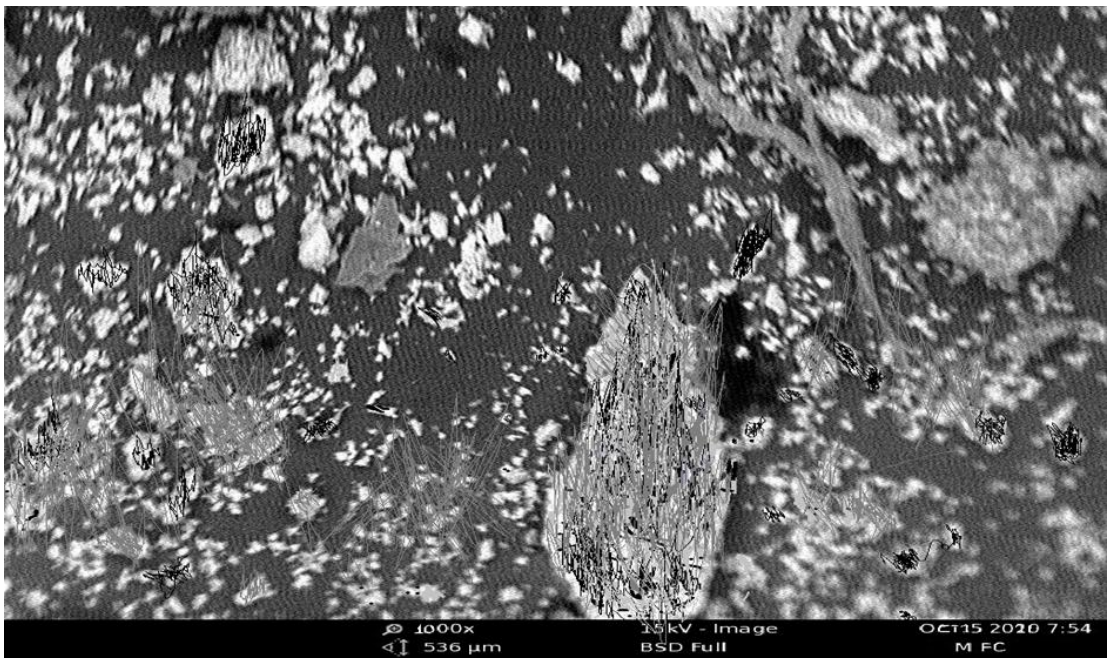

Figure 2 Scanning Electron Micrograph of MFC

Overall, FTIR and SEM confirmed that the composite (MFC) was essentially identical to the feldspar (FS) starting material; a tectosilicate with only slight modification. These observations were reported in a similar studies by (Awala and El-Jamal, 2011; Unuabonah *et al*., 2013 and Yazdani *et al*., 2014, Sanusi *et al*., 2016).

3.2. Effect of operating parameters on metal adsorption

3.2.1. Effect of initial metal concentration metal adsorption

The results of the influence of initial metal concentration on the percentage adsorption of As (III) ions onto the MFC adsorbent at pH 5 is shown in Figures 3 (a and b).

Decrease in percentage removal of the metal ions on the adsorbents with increase in initial metal ion concentration was observed. In fact, with increase in initial metal concentration after 100 mg/L, the percentage removal of As (III) ions by MFC adsorbent decreased from 99.98 to 68.16%. The decrease in percentage adsorption with increase in metal ion concentration is due to the fact that at lower concentrations, more of the metal ions would be removed by the abundant active sites on the surface of the adsorbents. However at higher metal ion concentrations, less metal ions were adsorbed due to the saturation of the available active adsorption sites on the adsorbent surface preventing further metal ion binding hence the adsorption percentages decrease (Ozdes *et al*., 2011). This implies that if the concentration is significantly increased further, a corresponding decrease in percentage removal would be expected due to complete saturation of the active sites. Similar result has been reported (Das and Mondal, 2011).

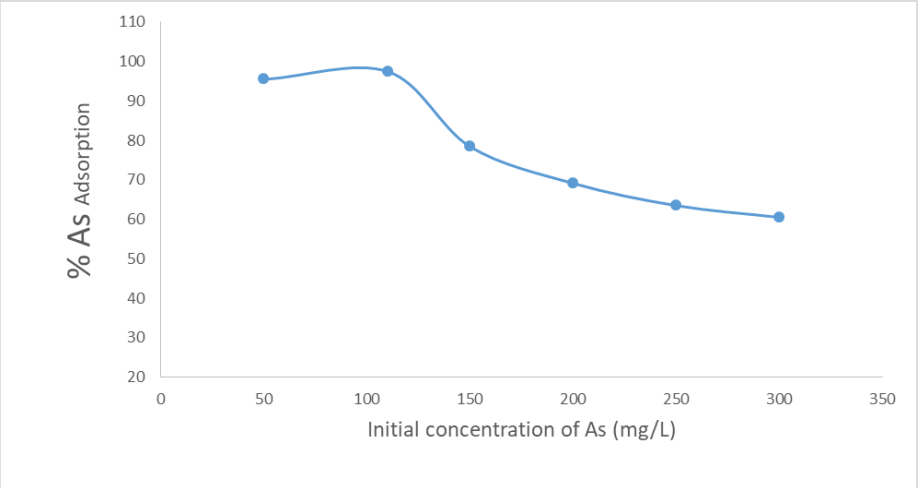

Figure 3a Effect of initial metal concentration on the adsorption of As (III) ions onto MFC

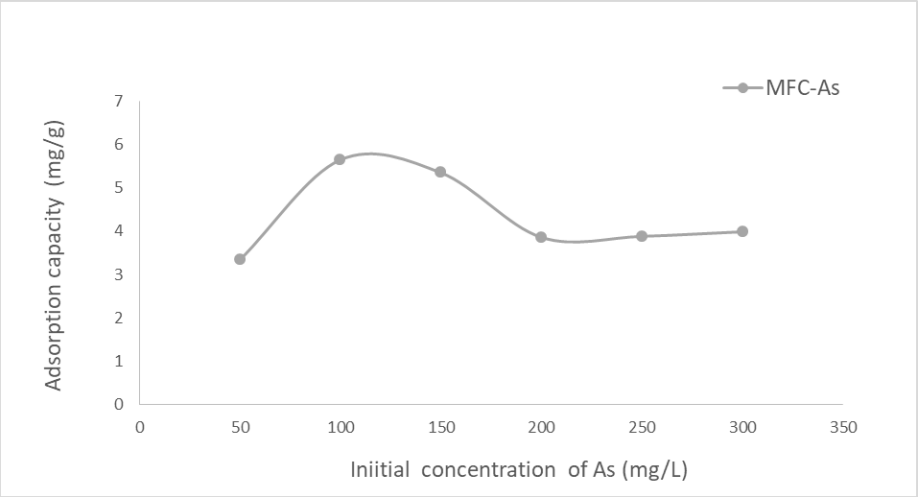

Figure 3b Effect of initial metal concentration on the adsorption capacity of MFC adsorbent for As (III) ions in aqueous solution

The influence of metal concentration on the adsorption (uptake) capacity of the adsorbents for Pb (II) and Cd (II) was also determined as illustrated in Figures 3 (c and d). However, unlike the decrease observed in percentage adsorption, an increase in adsorption capacity for the ions on all the adsorbents with increase concentration was recorded. With increase in metal ion concentration from 50 to 300mg/L, an increase in the adsorption uptake capacity of As (III) onto MFC from 3.817 to 5.650 mg/g. The increase in uptake capacity observed might be attributed to increased concentration which generated an increase in driving force of the metal ions towards the active adsorption sites, overcoming mass transfer resistance between aqueous and solid phase (Adebowale *et al*., 2005). Therefore, higher concentration of metal ions in solution implied that more amount of metal ion would be adsorbed per unit mass of the adsorbent with maximum utilization of the active binding sites (Hossain, 2013). Similar result has also been reported (Chukwuemeka-Okorie *et al*., 2018; Ogbu *et al.,* 2019).

3.2.2. Effect of contact time As (III) adsorption

The results of the effect of contact time on the adsorption of As (III) ions onto MFC was presented in Figure 4. It was observed that As (III) ions uptake was rapid within (15-30 min), afterward it continued at a slower rate and finally reached equilibrium in 120 minutes. After equilibrium is reached, there was little or no adsorption (marginal uptake) till 300 minutes. Further increase in contact time beyond the equilibrium time had no significant effect on the amount of As (III) ions adsorbed. The equilibrium percentage adsorption of As (III) ions by the novel bio-based composite adsorbent was 99.90% at equilibrium contact time of 120 min. The presence of more vacant adsorption active sites at the surface of MFC adsorbent accounted for the initial rapid arsenic uptake, afterward the metal ion adsorption progressed slowly and finally attained equilibrium at 120 minutes when the active adsorption sites has been saturated. Similar observation on the effect of contact time on the two metal uptake was reported (Sanusi et al., 2016). The faster rate of adsorption of As (III) by the adsorbent is due to the smaller ionic radii of As (III) (0.064 nm) which made its diffusion faster to the surface of adsorbents than other larger-sized metal ions (Rafatullah *et al.,* 2013).

From the batch adsorption experiment, an optimum contact time of 120min was used in this study to ensure that accurate equilibrium adsorption of the arsenic ions onto the MFC adsorbent was attained.

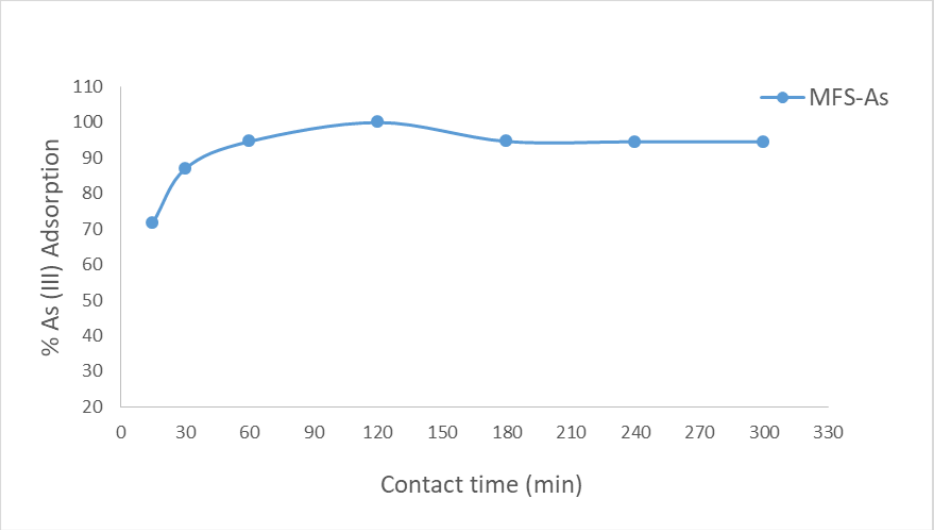

Figure 4 Effect of contact time on the percentage adsorption of As (III) ions onto MFC

3.2.3. Effect of temperature on As (III) adsorption

Figure 5 showed equilibrium adsorption trend as with respect to temperature of the aqueous solution. It was observed from the plot that increase in temperature from 308 to 328^{0}K, did lead to a significant decrease in adsorption of As (III) ions by MFC adsorbent from the aqueous solution. as solution temperature increased from 308 to 328^{0}K. The results indicated that at lower temperature of 308^{0}K the metal uptake is 96.58% which favours the adsorption of As (III) ions onto the novel bio-based composite adsorbent. The improved adsorption capacity of MFC for As (III) with decrease in temperature suggested that the adsorption of As (III) followed an endodermic process. The reason might be due to the dissociation of some active sites on the adsorbent's surface which created a hindrance for the adhesion of the metal ions onto the MFC surface (Ogbu *et al*., 2019; Chukwuemeka-Okorie *et al*., 2018).

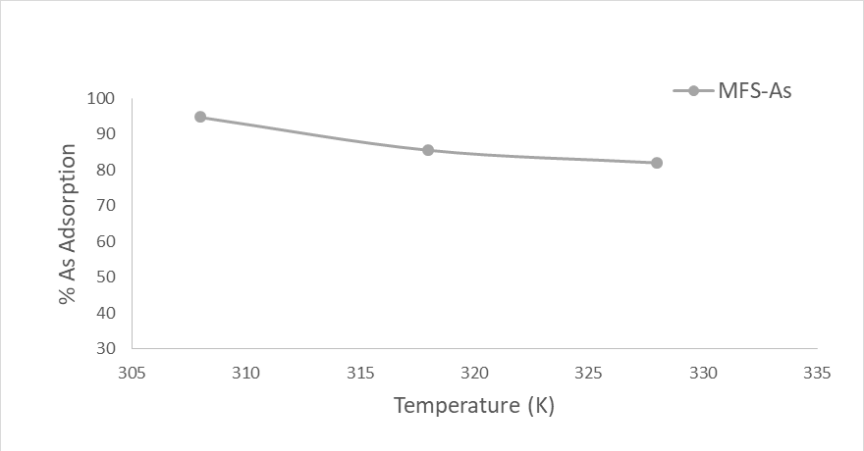

Figure 5 Effect of temperature on the percentage adsorption of As (III) ions onto MFC

3.2.4. Model Development for Optimization of As (III) Adsorption

In this experimental study, the central composite design (CCD) method as presented in Table 3 was applied to design experiments, propose empirical models, investigate the interaction effects of the three factors (adsorption variables) and determine the optimum values for the studied operating variables (initial metal concentration, contact time and temperature) to achieve the maximum response (adsorption efficiency of As (III) in aqueous solution (Yazdani *et al.,* 2013; Singh and Bhateria, 2020).

The models (in actual form) for arsenic ion uptake as presented in equations 2 were employed to analyze the effect of the independent variables on adsorption amount (*Y*). The results revealed that pH, adsorbent dosage, contact time and metal concentration presented the most significant effects on the metal adsorption. A positive sign coefficient term indicating the variables affecting metal uptake positively (synergetic effect) while negative sign coefficient terms are suggestive of uptake been antagonistic effect (decrease) on response values predicted by the quadratic model equations (Yazdani *et al.,* 2013).

As (II) Removal %

$$Y_3 = 27.11 + 0.61C_o + 0.04C_o^2 + 0.15D - 0.06D^2 - 2.25pH + 1.35pH^2$$

$$-1.09T + 0.12T^2 + 1.09CoD - 0.58CopH - 0.28CoT$$

$$+ 0.16DpH + 0.35DT + 0.10\ pHT. \quad (16)$$

The results of the statistical analysis and significance test for the model applied were obtained from analysis of variance (ANOVA) as displayed in table 6 (a and b). A higher *F* value indicates a greater significance of most of the variables in the response indicated in model regression equations. Most of the probability (p values) of the models are less than 0.05 which indicated that they are statistically significant (s) while those greater than 0.05 are insignificant (n) indicated as superscript on the values shown in Table (6a and b). Those significant values were further confirmed by the high R2 of the models (Adetokun et al., 2018). The optimum variables predicted by the model and that of experimental results for maximum uptake of the four metals were presented in table 7 (a and b). These were further validated by comparing experimental results to the predicted results. Higher coefficients of determination i.e. adjusted R2 (0.9959), is in good agreement with the predicted R2 (0.9981) as shown in table 7 (a and b) signifying less variation between the predicted and actual values (Adetokun et al., 2018). The results confirmed the adequacy of the selected quadratic model (Singh and Bhateria, 2020).

Table 3 Design of experiments for adsorption of As (III) on MFC using central composite design (CCD)

Run order	**Adsorption Parameters**			**Responses**	**CCD Position**
Run order	Initial concentration (mg/L)	Temperature (^{0}K)	Contact time (min)	Adsorption efficiency (%) As (III)	CCD Position
1	100	300	30	75.01	Axial
2	75	318	60	79.55	Factorial
3	50	328	120	63.45	Factorial
4	150	315	60	67.79	Factorial
5	125	300	210	54.77	Factorial
6	100	308	60	97.58	Central
7	100	308	120	99.72	Central
8	100	308	120	99.98	Central
9	100	328	60	94.73	Central
10	50	308	180	86.69	Axial
11	150	315	210	62.98	Axial
12	50	328	30	96.98	Axial
13	75	300	30	90.43	Factorial
14	125	318	30	78.61	Axial
15	150	315	60	67.79	Factorial
16	100	308	120	99.98	Central
17	125	300	210	54.77	Factorial
18	100	308	60	97.58	Central
19	100	328	60	94.73	Central
20	75	308	180	86.69	Axial

3.2.5. Validation of the Models for optimization

The model validation was carried out through performing four experiment sets with different combinations of the process variables and the response values (Y, mg/g) were determined using the coded values of the process variables as shown in (Table 3) above. A good correlation of determinations ($R^2 \geq 0.99$) from the response surface plot of the predicted results against experimental (actual) results of the adsorption variables as shown in Figure 6, and the good agreement between the Y_{pred} and Y_{exp} values as shown in Table 5 (a and b), have demonstrated the adequacy of the models applied to predict the response results and hence the model validation in the optimization process (Adetokun *et al.,* 2018). The model summary statistics and adequacy test results are summarized in Table 4. The lack of fit of the model was found to be insignificant for the selected metal ions adsorption onto the adsorbent. Hence, the effect of interactions of independent adsorption variables on the responses are adequately described by the quadratic regression equation models for As (III) with R^2 >0.99. The standard deviation of the residuals were found to be 13.67 with small pure errors for As (III) ions respectively. The "adeq precision" of the model was 40.31 at (adeq > 4) for As (III) ions respectively. The results showed that the value of noise ratio of the model are in the desirability range of 0.987. Similar statistical results for optimization of metal adsorption was reported in a research work by (Singh and Bhateria, 2020).

Table 4 Analysis of variance (ANOVA) for As (III) adsorption onto MFC Adsorbent

Response	Source	Sum of Squares	df	Mean Square	F Value	P- Value Prob > F	Comments
As (III)	Model	2590.56	14	185.05	953.48	<0.0001	SD = 0.69
Removal	Initial conc. (C_0)	100.00	1	100.00	241.06	<0.0001	Mean = 21.02
	Time (T)	120.00	1	120.00	0.66	<0.0001^S	CV = 3.62
	Dosage (D)	50.21	1	50.21	105.33	0.0555^n	R^2_{pred} = 0.9981
	D-pH	121.82	1	121.82	98.12	0.0519	$R^2_{(adj)}$ = 0.9959
	C_0T	115.73	1	115.73	4.83	0.1900	AP =40.31
	C_0D	120.14	1	120.14	5.01	0.1051^n	
	TD	196.13	1	196.13	2.01	0.1900	
	C_0^2	300.00	1	300.00	3.25	0.1051	
	$C_0{}^2T$	237.28	1	237.28	9.90	0.0118	
	$C_0{}^2D$	583.33	1	583.33	30.13	0.0004	R^2 = 0.9960
	Residual	83.61	16	13.67			
	Lack of fit	1.15	12	0.10	0.16	0.9910	Not significant
	Pure error	1.76	3	0.590			
	Cor. total	2593.58	29				

S: significant; n: insignificant; df: degree of freedom; SD: standard deviation; CV: coefficient of variance; R^2: correlation of determination; AP: adequate precision.

3.2.6. Response Surface Plotting

Three-dimensional surface plots presented the individual and interactive effects of independent variables, namely, pH, initial metal concentration, contact time and adsorbent dosage on the adsorption efficiencies and capacities of As (III) i.e. the response values as predicted by the models. The combined effect of interaction of initial metal concentration and adsorbent dosage shown in Figures 7 (a-c), indicated the significant influence of both factors on the adsorptive behaviour of As (III) onto MFC adsorbent. For all the metal ions, while the removal percentage increased with increasing adsorbent dosage, this was due to the presence of more active adsorption sites and large adsorbent surface area that is readily available for metal uptake (Adetokun *et al*., 2018; Sanusi *et al.,* 2016). On the contrary, the removal percentage was reduced by increasing the initial metal concentration. This observation might be due to the limited active sites on the adsorbent surface which become saturated at high adsorbate concentrations (Ozde *et al.,* 2011). More so, the removal of metal ions onto MFS was increased as the contact time increased from (30 to 60 min) for of As (III) ions. These results confirmed that the initial metal adsorption rate was very rapid due to the availability of large surface area and the presence of unused sites on the adsorbent surface (Ogbu *et al.,* 2019). The slow rate of metal ion removal after equilibrium time might be due to the difficulty of the metal ions in reaching the remaining vacant adsorbent active sites, a resultant of barrier factor i.e. repulsive forces (Akpomie and Dawodu, 2014). As seen in Figures 7 (a-c), the response surface diagram for the interactive effect of the adsorbent dosage, initial metal concentration and the initial pH showed that the metal adsorption by the MFC extremely depends on the pH of the solution. Pb (II) removal at lower pH is lower than the metal removal at higher pH in the experimental pH range. As has already been mentioned, at the lower pH, there are great number of protons in the aqueous solution which compete with the metal ions. Conversely, at the higher pH, there are a considerable number of OH^- in the aqueous medium which enhanced metal adsorption. Therefore, the adsorbent can provide more negative charges in very low acidic or alkaline medium rather than at higher acidic medium, and since the metal ions are cationic in nature, removing them from the alkaline solution would be much easier. In addition, it could be seen that the change of adsorbent dose and initial metal concentration do have a significant interactive effect on metal removal efficiency and capacities even at different pH 5.

The optimum values of experimental (actual) and the maximum values predicted responses are presented in Table 5 (a and b). The maximum removal percentages for As (III) were predicted to be 99.72 %, respectively. Verification experiments were conducted under the optimum conditions, and the removal percentages were 99.98% and 96.24%

for As (III) respectively at adsorbent dose of 1g, initial metal concentration (100mg/L) and temperature (308◦K). These experimental results were similar to the predicted values and indicated the suitability, accuracy and adequacy of the models used. The metal uptake capacities for the metals obtained under the optimum experimental conditions were 5.504 mg/g for As (III) while the predicted values for As (III) were 5.535 mg/g.

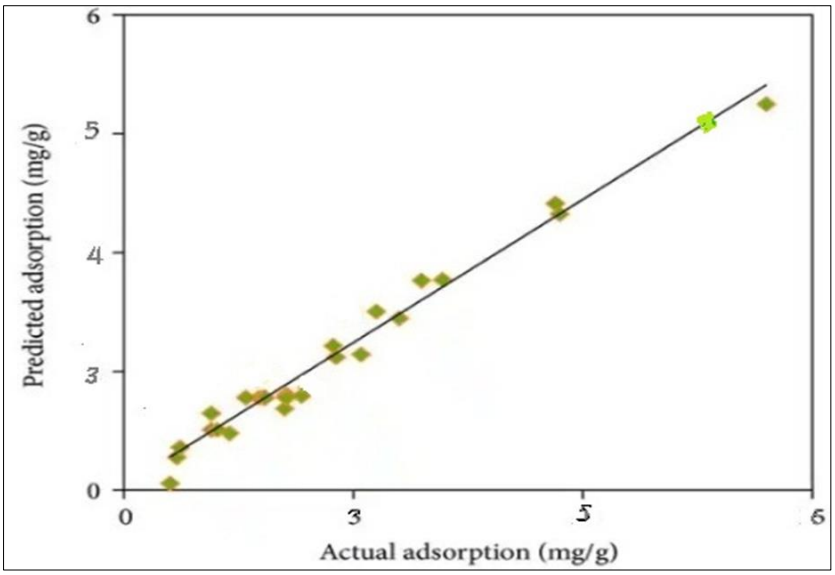

Figure 6 Plot of predicted and actual adsorption capacity (mg/g) of As (III) ions onto MFC

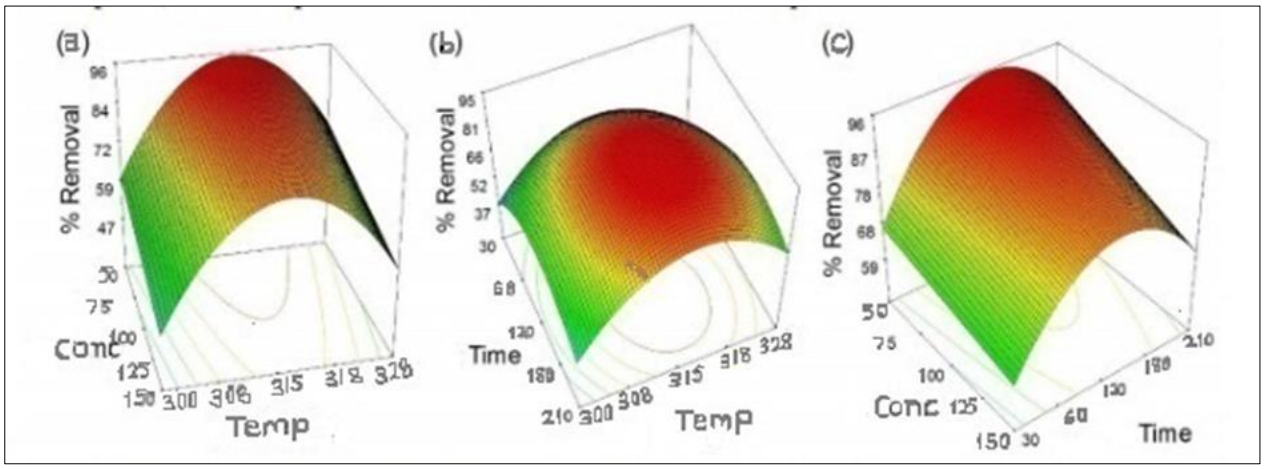

Figure 7 Response surface plot for As (III) ions removal by MFC adsorbent

3.2.7. Adsorption Process Optimization

The main objective of the present work was to reach the most effective values of process variables for the optimization of As (III) adsorption onto the MFC composite from aqueous solution. This aim was fulfilled using the quadratic model within the studied experimental range of the selected parameters. The optimization of the selected adsorption parameters at optimum values of pH 5, temperature 308◦K, initial metal concentration 100mg/L, and adsorbent dose 0.5 g revealed the maximum metal uptake capacities (predicted values) of 14.021 mg/g and 3.128 mg/g for As (III) in aqueous solution. Correspondingly, the experimental values of the metal adsorption under the optimum condition of the process parameters were obtained as (14.148 mg/g and 3.504 mg/g) for the selected metal ions (Table 7a). It should be noted that the experimental and predicted results of metal adsorption efficiency onto MFC at optimum variables values was determined as (99.98%, 99.95%) for As (III) ions as shown in (Table 7b).

Table 5a The model validation results for predicted and experimental maximum values of As (III) adsorption capacity onto MFC obtained in optimum conditions

Exp. No	Time (T)	Temp (^{0}K)	Metal conc. (mg/L)	Adjusted R^2	Predicted R^2	Metal conc. (mg/L)	Adsorption capacity (mg/g)
							Exp. Pred.
As (III)	120	308	100	0.9986	0.9996	100	5.650 5.535

Table 5b The model validation results for predicted and experimental maximum values of As (III) removal percentages obtained in optimum conditions

Heavy Metal	Time (min)	Temp (^{0}K)	Metal conc. (mg/L)	Adjusted R^2	Predicted R^2	Adsorption Model (%)
						Exp. Pred. desirability
As (III)	120	308	100	0.9986	0.9996	99.98 99.95 0.987

3.2.8. Adsorption Isotherm Studies

The equilibrium adsorption isotherms are one of the most important data that provide information on surface properties of adsorbents, adsorption mechanism and sorbents affinity (Das and Mondal, 2011). The relationship between the amount As (III) ions adsorbed onto the adsorbents (MFC) and its equilibrium concentrations in aqueous solution were evaluated using of Langmuir and Freundlich models. The equilibrium data obtained from the adsorption of As (III) ions onto MFC were fitted to Langmuir and Freundlich isotherm models as shown in Figure 8 (a and b). All of the isotherm parameters, constants and correlation coefficients were calculated from the linear equations of the models and shown in Table 6. According to the Langmuir isotherm model, the maximum monolayer adsorption capacity of MFC for As (III) was found to be large indicating As (III) ions was well adsorbed onto adsorbent's surface. The *b* values of As (III) was 0.064, confirming that metal ions have high affinity to the bonding active sites of the adsorbent surface than the many metal ions (Ozdes *et al*., 2011)

From 50 and 300 mgL^{-1} of metal ions concentration, the R_L values ranged from 0.531 to 0.910 for As (III) ions which then approached zero with increase in the C_o values of the metal ions. The values of R_L indicated that As (III) adsorption onto MFC is favorable under optimum conditions. Furthermore n values obtained from Freundlich isotherm model for the metal ions were higher than unity which supported the favourability of adsorption process. By comparing the correlation coefficient values obtained from Langmuir and Freundlich isotherm models for the metal ions, it could be observed that the Langmuir isotherm model was best fitted for As (III) ions removal from aqueous solution with R^2 greater than 0.99. This observation might be due to both homogeneous distribution of adsorption active sites on the surface of novel MFC adsorbent. Similar observation was reported (Adebowale *et al*., 2005; Ozdes *et al*., 2011; Unuabonah *et al*., 2013).

Table 6 Adsorption Isotherm Parameters for adsorption of As (III) ions onto MFC adsorbent

Metal Langmuir	As (III)	Freundlich	
q_m (mg/g)	88.49	K_F	8.916
b (L/mg^{-1})	0.064	1/n	0.281
R_L	0.910	n	3.557
R^2	0.9998	R^2	0.8795

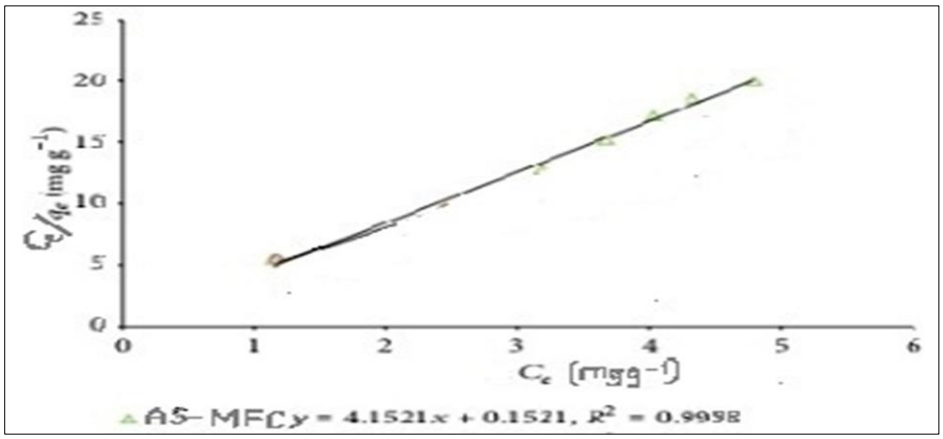

Figure 8a Langmuir isotherm plots of adsorption of As (III) ions onto MFC adsorbents

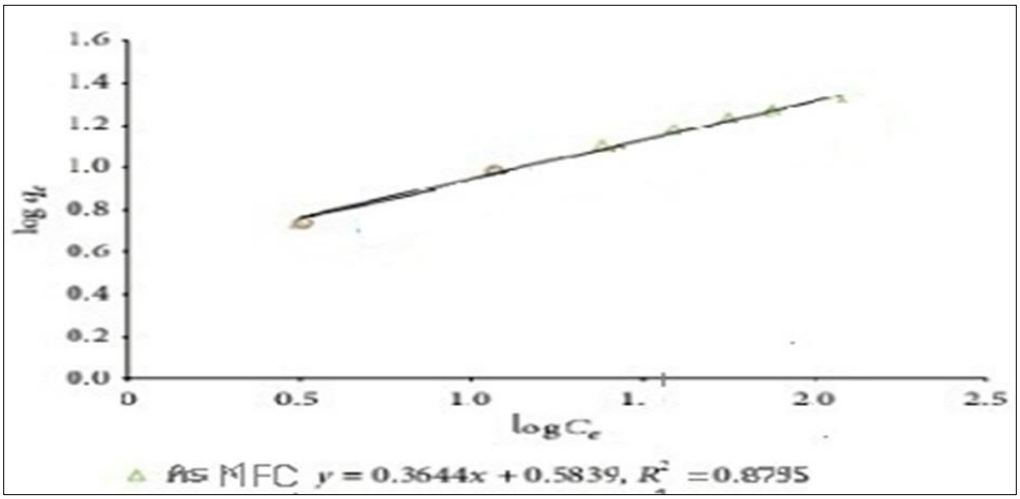

Figure 8b Freundlich isotherm plots of adsorption of As (III) ions MFC adsorbents

3.3. Adsorption Kinetic Studies

Kinetic modeling evaluates adsorption mechanism, which include mass transfer, chemical reaction and diffusion control (Ogbu *et al*., 2018). The metal ions uptake was rapid for the first 30 min because at the beginning of the adsorption the active adsorption sites on the adsorbent surface were more available thus metal ions could interact easily with these sites. Afterward it continued at a slower rate and finally reached to the equilibrium by virtue of the saturation of adsorption sites on adsorbent surface within 120 min.

Four adsorption kinetics models were employed to investigate the mechanism and rate of the adsorption process. These are the Lagergren pseudo-first-order (PFO), pseudo second-order (PSO), Elovich and intra–particle diffusion (IPD) kinetic models. The parameters for each kinetic model and its correlation coefficients (R^2) for the adsorption As (III) ions unto the adsorbents are shown in Table 7. Plots of the four kinetic models are shown in Figure 9 (a - d). The q_e and rate constants were calculated from the slope and intercept of the plots of log $(q_e - q_t)$ *vs. t*; and *t/q vs. t* for PFO and PSO respectively.

From the PFO R^2 values obtained, it was observed that the model did not show good fit to the adsorption of As (III) ions onto MFC adsorbents; as the R^2 values were lower than 0.9. The observation was validated by the values of the q_e exp which showed a great discrepancy with the q_e cal of the PFO model for As (III) ions. Moreover, the experimental results of As (III) removal by MFC from the aqueous solution best fitted the pseudo-second order model, with the correlation of the coefficient close to or equals unity ($0.99 < R^2 \leq 1$). Furthermore, results of PSO models showed that the values of q_e cal were closer to the values of q_e exp than those obtained from the PFO model shown in Table 7. However, the low values of the regression coefficient ($R^2 = 0.8317 – 0.8845$) of the Elovich kinetic model coupled with the lower values of

the Elovich constants, α (mg g^{-1} min^{-1}) and β (gmg^{-1}) as shown in Figure 9 (a - d) suggested that kinetic data did not follow the Elovich model. Similar results have been reported (Adebowale *et al*., 2005; Das and Mondal, 2011; Chukwuemeka-Okorie *et al*., 2018).

From equation 10, a plot of q_t vs $t^{1/2}$ should be a straight line with a slope k_i and intercept C when the adsorption mechanism is in line with the intra-particle diffusion process. The intra-particle diffusion process, though not the only rate-limiting step is the predominant in the metal adsorption onto MFC, as the plot did not pass through the origin (Olu-Owolabi *et al*., 2016, Sanusi *et al*., 2016). Furthermore, the occurrence of the intercept C, showed the involvement of surface active sites on adsorption process (Yazdani *et al*., 2013). The metal ions on adsorbent surfaces diffuse inward into the porous surface and thus follow the IPD mechanism (Das and Mondal, 2011). A significant adsorption of As (III) ions was achieved during movement of adsorbates from solution to adsorbents surface indicating the conformity of metal uptake process to the IPD model (Chukwuemeka-Okorie *et al*., 2018).

By evaluating the intra-particle mass transfer curve, it was observed that the As (III) adsorption process was found to be followed by two distinct phases. The first phase is attributed to the diffusion of metal ions through the solution to the external surface of MFC while the second phase indicated the intra-particle diffusion (IPD) of As (III) ions into the pores of the adsorbents. The intra-particle rate constants for the first phase (k_{id}, 1) and second phase (k_{id}, 2) and C parameters were obtained from the plot of qt versus $t^{1/2}$ and the results were given in Table 7. By comparing the rate constants, the lower values of (k_{id} 2) than (k_{id} 1) indicating that the rate limiting step for As (III) adsorption process is intra-particle diffusion. As observed, all the R^2 values obtained for IPD for the metal ions were greater than 0.9. This implies that film diffusion (surface phenomenon) also played a dominant role in the adsorption process. As a result, As (III) uptake by MFC is considered complex process as intra-particle diffusion and surface adsorption contributed to the rate limiting step (Ozdes et al., 2011).

Table 7 Adsorption Kinetic Parameters for As (III) adsorption onto MFC adsorbent

Metal/ Kinetic Models	**As (III)**	**MFC**	
Pseudo-first order (PFO)	Values	Pseudo- second order (PFO)	Values
q_e exp (mg/g)	26.54	q_e exp (mg/g)	26.54
q_e cal (mg/g)	45.60	h (mg/g min)	0.999
K_1 (min^{-1})	0.018	K_2 (g/mg min)	3.94×10^{-3}
R^2	0.9889	q_e cal (mg/g)	26.54
		R^2	1.0000
Elovich	Values	Intraparticle diffusion (IPD)	Values
α (mg/g min)	5.291	K_{id} 1 (mg/g $min^{1/2}$)	2.554
β (g/min)	0.128	K_{id} 2 (mg/g $min^{1/2}$)	1.490
R^2	0.8345	C	18.106
		R^2	0.9995

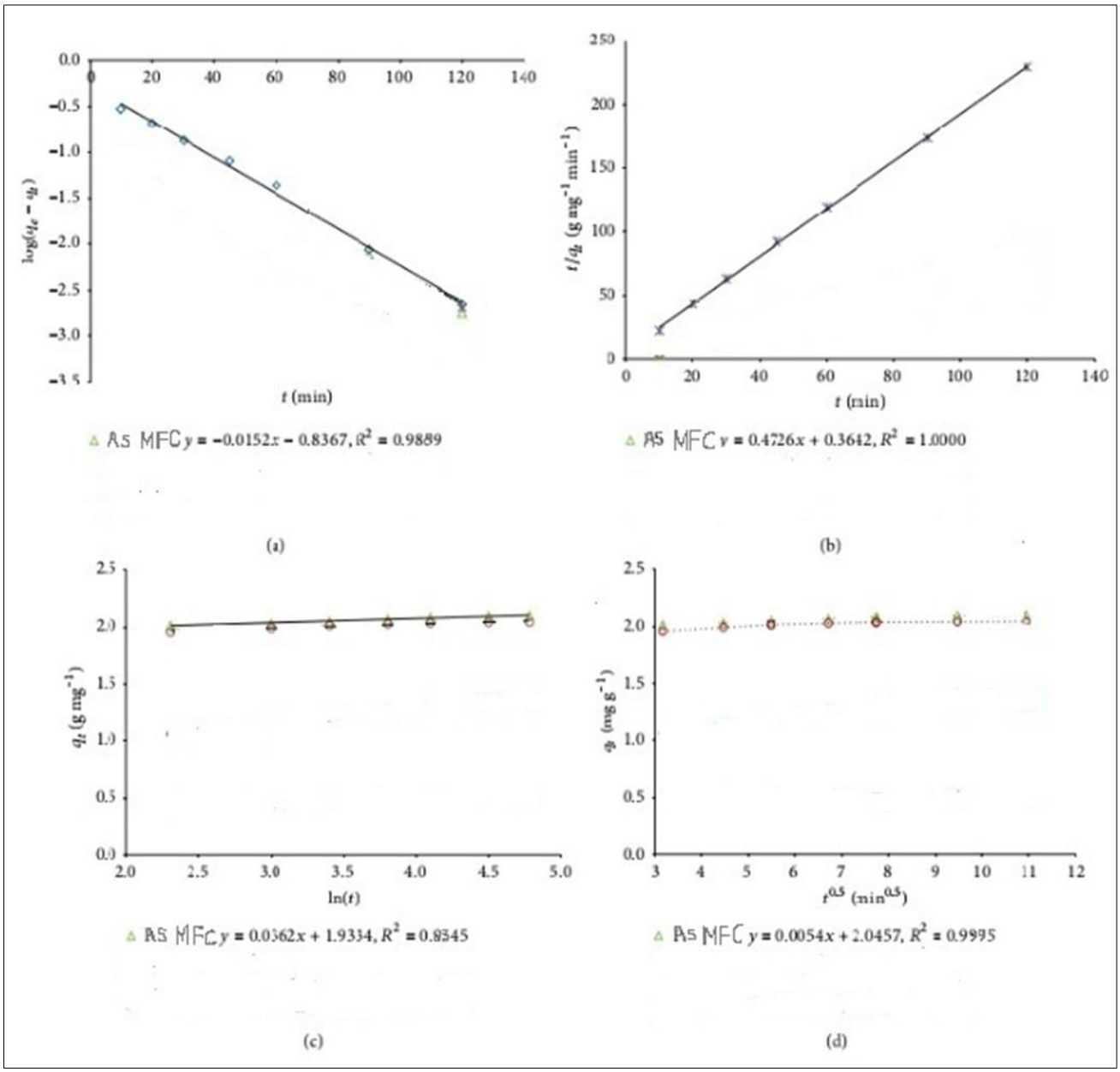

Figure 9 (a) PFO kinetic plots (b) PSO kinetic plots (c) Elovich plots and (d) Intraparticle diffusion plots of As (III) adsorption onto MFC adsorbents

3.4. Effect of temperature and thermodynamic studies of metal adsorption

Adsorption efficiency of MFC removal of As (III) ions from Aqueous solution decreased from 5.650 mg g^{-1} (99.98%) to 3.187 mg g^{-1} (68.57%) for As (III) ions as the temperature was increased from 308 to 328 ^{0}C, indicating that the adsorption process for the metal ions followed exothermic process (Ozdes *et al*., 2011). The thermodynamic parameters, enthalpy change (ΔH^0), entropy change (ΔS^0) and standard free energy (ΔG^0), denote the features of the final state of the system. The ΔG^0, ΔH^0 and ΔS^0 values were calculated to evaluate the feasibility of adsorption. The calculated thermodynamic parameters of adsorption are given in Table 8.

The negative values of ΔG^o obtained for As (III) ions at all temperatures as shown in Table 8, suggested the feasibility of the adsorption process and spontaneous nature of the adsorption of all the metal ions onto MFC adsorbents (Ozdes *et al*., 2011). Moreover, the decrease in the magnitude of negative ΔG^o values with an increase in temperature indicated an increased feasibility of adsorption (better metal uptake) of As (III) ions at lower temperature in Table 8. The observation is corroborative to the earlier reports (Ozdes et al., 2011; Dawodu and Akpomie, 2014). The negative ΔH^0 values obtained for the As (III) ions on MFC indicated an exothermic process which was suggestive of physisorption adsorption (Dawodu and Akpomie, 2014). The magnitude of the enthalpy change (ΔH^o) provides information about the type of

adsorption. In addition, the extent of enthalpy value gives indicative information on the type of metal adsorption, which can be either physical or chemical. The enthalpy change (ΔH^o) in the range of 2.1–20.9, 20.9–80.0, and 80.0–418.4 $kJmol^{-1}$ is indicative of physisorption, combination of physisorption and chemisorption, and chemisorption, respectively (Rahman and Sathasivam, 2015). From table 8, the value of ΔH^o for As (III) was -16.58 for MFC adsorbent, indicating physisorption and exothermic process (Ogbu *et al*., 2019). Physical adsorption is desirable because there is a lower energy barrier to be overcome by metal ions, which allows easy desorption from the surface of the adsorbent during recycling (Das and Mondal, 2011; Dawodu and Akpomie, 2014; Rahman and Sathasivam, 2015). The positive ΔS^0 values suggested an increase in the randomness at the solid/solution interface during the adsorption of As (III) ions onto MFC on the active sites of the adsorbents. Similar observations were reported in related metal adsorption studies (Rahman and Sathasivam, 2015; Yazdani *et al*., 2013; Chukwuemeka-Okorie *et al*., 2018)

Table 8 Thermodynamic parameters for the adsorption of As (III) onto the MFC adsorbent

Parameter/ Temperature (^0K)	**MFC**
As (III)	
ΔH^0 ($kJmol^{-1}$)	-16.58
ΔS^0 ($J/mol^{-1}K^{-1}$)	42.65
308^0K (ΔG^0)($kJmol^{-1}$)	-7.52
318^0K (ΔG^0)($kJmol^{-1}$)	-8.34
328^0K (ΔG^0)($kJmol^{-1}$)	-9.48
328^0K (ΔG^0)($kJmol^{-1}$)	-3.96

4. Conclusion

In this study, MFC biobased composite adsorbent was synthesized, characterized, and tested for the removal of As (III) ions from aqueous solution. A four-factor central composite design (CCD) accompanied by response surface methodology (RSM) was used for the optimization of adsorption parameters on the metal uptake by the adsorbents. The results showed that the predicted values obtained under the optimum conditions pH 5, temperature 300°K, initial metal concentration 100 mg/L, and dose 0.5 g) were close to the experimental values for As (III) ions. Furthermore, the results from isotherm studies showed that As (III) ions adsorption onto the adsorbent was best fitted to the Langmuir isotherm model, hence chemisorption process. The results of the kinetic studies showed that the adsorption process for As (III) ions followed pseudo second order kinetic model. The Intraparticle diffusion though not the only rate- rate controlling step, played important role in the metal ions uptake by the adsorbents. However, the modified feldspar composite (MFC) showed a fastest rate of metal ions removal in the aqueous solution. From thermodynamic studies, As (III) ions adsorption process was feasible, spontaneous, and exothermic process. However, the results obtained indicated that As (III) ions adsorption process onto the MFC was a complex one involving more than one mechanism suggestive of the presence of heterogeneous active sites on MFC surface. From this research it was discovered that the synergestic combination of feldspar with *Theobroma cacao* pod and the calcination have improved MFC adsorption capacity. Therefore, the environmentally friendly modified feldspar composite (MFC) has the potential for better performance as adsorbent for As (III) in aqueous solutions and possible application in wastewater treatment.

Compliance with ethical standards

Disclosure of conflict of interest

No conflict of interest.

References

[1] Adebowale KO, Unuabonah IE, Olu-Owolabi BI. The effect of some operating variables on the adsorption of lead and cadmium ions on kaolinite clay. Journal of Hazardous material. 2005; 134: 130-139.

[2] Adetokun, Abdulmalik A, Sani Uba, Zaharaddeen N Garba. Optimization of adsorption of metal ions from a ternary aqueous solution with activated carbon from Acacia senegal (L.) Willd pods using Central Composite Design. Journal of King Saud University – Science. 2018; 31: 1452-1462.

[3] Akpomie KG, Dawodu FA. Montmorillonite-rice husk composite for heavy metal sequestration from binary aqua media: a novel adsorbent, Transactions of the Royal Society of South Africa. 2014; 54: 32-39.

[4] Anusa R, Ravichandran C, Sivakumar EKT. Removal of heavy metal ions from industrial waste water by nano-ZnO in presence of electrogenerated Fenton's reagent. International Journal of Chem Tech Research. 2017; 10(7): 501-508.

[5] Awala HA, El Jamal MM. Equilibrium and kinetics study of adsorption of some dyes onto feldspar. Journal of Chemical Technology and Metallurgy. 2011; 46(1): 45-52.

[6] Brigatti MF, Lugli C, Poppi L. Kinetics of Heavy Metals and Recovery in Sepiolite. Applied Clay Science. 2011; 16(1-2): 45-57.

[7] Chiban M, Zerbet M, Carja G, Sinan F. Application of Low-cost Adsorbents for Arsenic removal: A Review. Journal of Environmental Chemistry and Toxicology. 2012; 4(5): 91-102.

[8] Chukwuemeka-Okorie Helen O, Peter N Ekemezie, Kovo G Akpomie, Chisom S Olikagu. Calcined Corncob-Kaolinite Combo as New Sorbent for Sequestration of Toxic Metal Ions from Polluted Aqua Media and Desorption. Frontiers in Chemistry. 2018; 273(6): 1-13.

[9] Dang VBH, Doan HD, Dang VT, Lohi A. A Study on Heavy Metal Adsorption Using Shrimp Shell. Journal of Bio-resources Technology. 2009; 10(5): 211-223.

[10] Dawood SA. Synthesis and Characterization of Biomass and Clay Mineral Based Adsorbents for the Removal of Cationic Dye and Metal Ion from Wastewater by Adsorption. Faculty of Science and Engineering, WA School of Mines: Minerals, Energy and Chemical Engineering. Thesis is presented for the Degree of Doctor of Philosophy of Curtin University. 2018; 57-69.

[11] Francis MM. Functionalized Geopolymers derived from Clay and Rice Husk Ash for Removal of Selected Heavy Metals and Methylene Blue from Aqueous Solution. A Thesis Submitted in Partial Fulfillment of the Requirements for the Award of the Degree of Doctor of Philosophy (Chemistry) in the School of Pure and Applied Science of Kenyatta University. 2018; 1-2.

[12] Horsfall M, Abia AA, Spiff AJ. Removal of Cu (II) and Zn (II) ions from wastewater by Cassava (Manihot esculenta Cranz) Waste Biomass. Africa Journal of Biotechnology. 2014; 2(10): 360-364.

[13] Hossain MA. Development of novel biosorbents in removing heavy metals from aqueous solution. PhD Thesis, School of Civil and Environmental Engineering, Faculty of Engineering and Information Technology, University of Technology, Sydney (UTS) Sydney, Australia. 2013; 57-65.

[14] Jimoh T, Egila JN, Dauda BEN, Iyaka YA. Preconcentration and removal of heavy metal ions from aqueous solution using modified charcoal. Journal of Environmental Chemistry and Ecotoxicology. 2011; 3(9): 238-243.

[15] Md. Sayedur Rahman, Kathiresan V Sathasivam. Heavy Metal Adsorption on toKappaphycus sp. From Aqueous Solutions: The Use of Error Functions for Validation of Isotherm and Kinetics Models. BioMed Research International, Hindawi Publishing Corporation. 2015; 1-13.

[16] Obike AI, Igwe JC, Emeruwa CN, Uwakwe KJ. Equilibrium and Kinetic Studies of Cu (II), Cd (II), Pb (II) and Fe (II) Adsorption from Aqueous Solution Using Cocoa (Theobroma cacao) Pod Husk. J. Appl. Sci. Environ. Manage. 2018; 22(2): 182 – 190.

[17] Ofomaja AE, Unuabonah EI, Oladoja NA. Competitive modeling for the biosorptive removal of copper and lead ions from aqueous solution by Mansonia wood sawdust. Journal of Bioresource Technology. 2007; 101(11): 3844-3852.

[18] Ogbu IC, Akpomie KG, Osunkunle AA, Eze SI. Sawdust-kaolinite composite as efficient sorbent for heavy metal ions. Bangladesh J. Sci. Ind. Res. 2019; 54(1): 99-110.

[19] Olu-Owolabi B, Oputu OU, Adebowale KO, Ogunsolu O, Olujimi OO. Biosorption of Cd2+ and Pb2+ ions onto mango stone and cocoa pod waste: Kinetic and equilibrium studies. Scientific Research and Essays. 2012; 7(15): 1614-1629.

[20] Olu-Owolabi BI, Alimoh H Alabi, Emmanuel I Unuabonah, Paul N Diagboya. Calcined bentonite-biomass composites for removal of aqueous metal ions. Journal of chemical and engineering technology. 2016; 4: 1379-1383.

[21] Ozdes Duygu, Celal Duran, Hasan Basri Senturk. Adsorptive removal of Cd(II) and Pb(II) ions from aqueous solutions by using Turkish illitic clay. Journal of Environ. Management. 2011; 92: 3082-3090.

[22] Rafatullah MO, Sulaiman R Hashim, Ahmad A. Adsorption of methylene blue on low-cost adsorbents: a review. Journal of Hazardous Material. 2010; 177: 70-80.

[23] Salih AM. The purification of industrial wastewater to remove heavy metals and investigation into the use of zeolite as a remediation tool. A thesis submitted in partial fulfilment of the requirements of the University of Wolverhampton for the degree of Doctor of Philosophy. 2017; 31-33.

[24] Sanusi KA, Babayo AU, Isyaka MS. Evaluation of the Application of Modified Feldspar Clay for Adsorption of Pb+2 and Cu+2 in Aqueous Media: Equilibrium and Thermodynamic studies. Journal of Environmental & Analytical Toxicology. 2016; 6(2): 02-09.

[25] Singh Rimmy, Rachna Bhateria. Optimization and Experimental Design of the Pb2+ Adsorption Process on a Nano-Fe3O4 Based Adsorbent Using the Response Surface Methodology. ACS Omega. 2020; 5: 28305−28318.

[26] Unuabonah IE, Olu-Owolabi BI, Adebowale KO, Ofomaja AE. Adsorption of lead and cadmium ions from aqueous solutions by tripolyphosphate-impregnated kaolinite clay. Journal of Colloids and surfaces. 2007; 82: 202-211.

[27] Unuabonah IE, Gunter C, Weber J, Lubahn S, Taubart A. Hybrid Clay: A New Highly Efficient Adsorbent for Water Treatment. Journal of Industrial and Engineering Chemistry. 2013; 132: 252-255.

[28] WHO. Guidelines for drinking water quality by World Health Organization, Geneva, Switzerland. 2000.

[29] Yazdani M, Bahrami H, Arami M. Preparation and Characterization of Chitosan/Feldspar Biohybrid as an Adsorbent: Optimization of Adsorption Process via Response Surface Modeling. The Scientific World Journal. 2014; 20(14): 1-13.